This article has been accepted for publication in a future issue of this journal, but has not been fully edited. Content may change prior to final publication. Citation information: DOI 10.1109/TSG.2016.2593667, IEEE Transactions on Smart Grid

Spatio-Temporal Coordinated V2V Fast Charging Strategy for Mobile GEVs via Price Control

Miao Wang, *Member, IEEE*, Muhammad Ismail, *Member, IEEE*, Ran Zhang, *Member, IEEE*, Xuemin (Sherman) Shen, *Fellow, IEEE*, Erchin Serpedin, *Fellow, IEEE*, and Khalid Qaraqe, *Member, IEEE*

***Abstract*—A vehicle-to-vehicle (V2V) energy swapping strategy can provide an alternative fast charging way for gridable electric vehicles (GEVs) to relieve the charging overload problem in the power system during peak-demand hours. The main challenges in designing an efficient V2V energy swapping strategy are i) to stimulate mobile GEVs to participate in an energy swapping transaction that balances supply with demand at aggregators, and ii) to achieve optimal energy utilization and individual GEVs' profits. In this paper, we present a novel smart grid architecture with enhanced communication capabilities for mobile GEVs, via a heterogeneous wireless network-enhanced smart grid. We propose an online V2V energy swapping strategy based on price control. Specifically, mobile GEVs with surplus energy are motivated by getting paid to contribute to a V2V energy swapping transaction at aggregators with energy-hungry GEVs. To evaluate the performance of the proposed V2V energy swapping strategy, a realistic suburban scenario is developed in VISSIM to track the GEVs' mobility using the generated simulation traces. Extensive simulation results are given to demonstrate the efficacy of the proposed V2V energy swapping strategy.**

I. Introduction

Electric vehicles (EVs) represent an effective approach for sustainable and eco-friendly transportation systems. In addition, EVs have great potential to save thousands of dollars for drivers across the vehicle lifetime [1]. The widespread adoption of EVs in the transportation system results in problems for charging EVs which are fully reliant on rechargeable batteries. A major challenge is the overloading problem of the power system, since EV loads is the burden on the existing grid assets resulting in higher system peak and overload, especially at the distribution system level [2]- [4]. The problem is more critical for the fast charging since it requires much higher power than the regular charging. Therefore, to avoid power system overload during peak-demand hours and improve energy utilization without additional deployment costs, load management strategies are applied to efficiently distribute the EV charging load. Several works in literature [5], [6] have investigated coordinated charging strategies for EVs, where EVs obtain energy from charging stations via grid-to-vehicle (G2V) transfers. However, G2V is restricted by the technical limitations of the power system when the charging demand is very high. Thus, more efficient and economical charging approaches should be explored.

In literature, gridable EVs (GEVs) represent EVs with bidirectional chargers [7], which enable the energy delivery from EVs to the grid through vehicle-to-grid (V2G) discharging. Moreover, through bidirectional chargers, the discharged energy from some GEVs can be used for charging other GEVs, referred to as vehicle-to-vehicle (V2V) energy swapping in this paper [7]. As shown in Fig. 1, the V2V energy swapping can be performed via interaction among GEVs. Specifically, energy can be directly transferred among GEVs at an aggregator [8], which is connected to the smart grid and controlled by the grid operator, to offload the heavy power demands. Through V2V energy swapping, the charging efficiency of GEVs can be improved with simple infrastructure requirements.

To the best of our knowledge, there is a lack of research work to investigate charging/discharging coordination strategies for mobile GEVs in a V2V scenario. However, such a model is very useful for mobile GEVs (e.g., electric taxis/buses) that may require charging while on the road or may seek revenues by assisting in charging other GEVs. Unlike conventional coordination strategies, a V2V strategy, besides coordinating charging for the GEVs that need energy, should motivate discharging of the GEVs with surplus energy. In the presence of a set of aggregators in the power grid, spatial and temporal charging/discharging coordination can be implemented for mobile GEVs, due to the spatial and temporal fluctuations associated with charging demands and discharging offers at different aggregators. Through spatio-temporal coordination, the total supply and demand can be matched. Moreover, for mobile GEV charging/discharging, the assigned aggregators must be within the range of individual mobile GEVs given the GEV's current locations and battery energy levels, due to the tension between the available energy in battery and energy required to reach an aggregator, which is referred to as range anxiety.

In this paper, we aim to employ the real-time information of mobile vehicle locations and available energy to design an efficient spatio-temporal coordinated V2V energy swapping strategy. The main contributions of this paper are:

- A heterogeneous wireless network-enhanced smart grid is proposed, by integrating vehicular ad-hoc networks (VANETs [9]) and cellular networks (4G-LTE [10]), to

M. Wang, R. Zhang and X. Shen are with the Department of Electrical and Computer Engineering, University of Waterloo, Canada (e-mail: {m59wang, r62zhang, sshen}@uwaterloo.ca).

M. Ismail and K. Qaraqe are with the Department of Computer Enginering, Texas A&M University at Qatar, Qatar (email: {m.ismail, khalid.qaraqe}@qatar.tamu.edu).

E. Serpedin is with the Department of Computer Engineering, Texas A&M University, USA (e-mail: serpedin@ece.tamu.edu).

This research work is financially supported by Natural Sciences and Engineering Research Council of Canada Collaborative Research and Development Grants, Canada. In addition, parts of this paper, specifically Sections III, IV, and V were made possible by NPRP grant # NPRP 9-055-2-022 from the Qatar National Research Fund (a member of Qatar Foundation).

This article has been accepted for publication in a future issue of this journal, but has not been fully edited. Content may change prior to final publication. Citation information: DOI 10.1109/TSG.2016.2593667, IEEE Transactions on Smart Grid

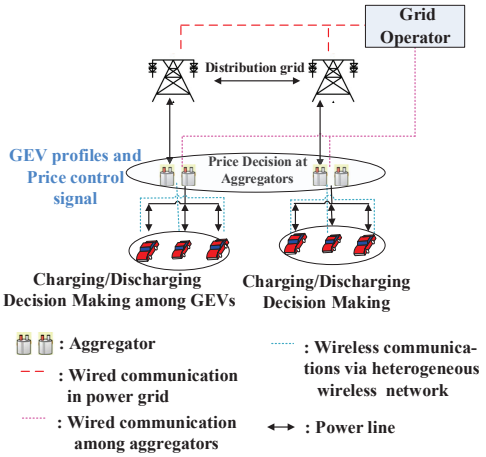

Fig. 1: Illustration of V2V energy swapping framework in the smart grid.

enable efficient collection of vehicular information and dispatch of the charging/discharging decisions to GEVs in a real-time manner.

- Based on the gathered information from both GEVs and the power grid, the aggregators determine the energy price for GEVs. The price control strategy is modeled as an Oligopoly game [11] with competition among GEVs.
- Using the announced price, a mobility-aware spatio-temporal coordinated V2V energy swapping strategy is designed to enable energy exchange among GEVs at the aggregators. The proposed strategy is modeled as a time-coupled mixed-integer non-linear programming (MINLP), which is decoupled into a series of sub-MINLPs through Lagrange duality [12]. Each sub-MINLP is further solved by the branch-and-cut-based outer approximation (BCBOA) algorithm [13].
- Extensive simulations are conducted to evaluate the performance of the proposed GEV energy swapping strategy. A realistic suburban scenario is developed in VISSIM [14], from which simulation traces are extracted.

Such a bidirectional energy swapping principle is not well studied in literature, and further investigation is required on optimal strategy design for joint fast charging and discharging of mobile GEVs from a game theoretic perspective. By considering the energy-excessive GEVs to supply the energy-hungry GEVs, our work finds an alternative and promising way to release the pressure on the power grid caused by peak-time GEV charging demands. The obtained results should shed the light on strategy designing for GEV fast charging/discharging in eco-friendly transportation systems as well as the economic interplay modeling between smart grid and individual GEVs.

The remainder of this paper is organized as follows. The related works are reviewed in Section II. The system model is presented in Section III. In Sections IV and V, the coordinated V2V energy swapping problem is formulated and solved, respectively. Section VI demonstrates the proposed strategy performance by computer simulations. Section VII concludes the paper. Mathematical proofs are given in the Appendix.

II. Related Work

In literature, several works have reported coordinated charging strategies of EVs. In [5], [6], [8], [15], [16], based on the collected information from the grid, the charging decisions are taken to improve the utilization of the power grid. All these works are designed for parked EVs, however, for mobile EVs, such decisions may cause a conflict between the system technical limitations and driver preferences, due to the range anxiety problem. For instance, some EVs can be charged only in the given nearby stations due to the existing battery levels and locations. However, the EV charging requests might be blocked due to the high charging loads present at the stations.

Through V2V transactions, high power demands can be offloaded from the power system to GEVs with excess energy to improve the GEVs' charging efficiency. Our objective is to design a mobility-aware V2V energy swapping strategy for mobile GEVs, with real-time vehicle information collection and decision dissemination through either cellular networks or VANETs. Our preliminary works [17] have investigated this problem by considering a single aggregator system without spatial coordinations. Another preliminary work [18] has proposed the basic idea to include the spatial coordination into the swapping strategy design. Building upon [17] and [18], this paper incorporates the spatio-temporal coordinations of the mobile GEVs into the optimization framework and describes the details of the proposed strategy.

III. System Model

In this section, first the heterogeneous wireless network and the transmission mechanism are introduced, leading to the heterogeneous wireless network-enhanced smart grid. Then, the power system model and individual GEV charging/discharging models are presented. In addition, the electricity price model is described. Finally, an overview of the proposed energy swapping strategy is shown.

A. Heterogeneous Wireless Network

To collect the information required by the energy swapping strategy in a real-time manner, the existing literature relies on cellular networks (e.g., GSM, 3G, LTE, etc.) [10], due to the large coverage area of base stations (BSs). However, as cellular systems are not dedicated for vehicular data collection, the associated cost will be very high, and may lead to numerous congestion for other cellular services.

VANETs, dedicated to vehicular communications, can be used for real-time information collection by deploying road-side units (RSUs) and equipping vehicles with on-board communication facilities (e.g., on-board units (OBUs)). Two communication modes can be adopted, namely, vehicle-to-RSU (V2R) communications and vehicle-to-vehicle (V2V) communications[1]. Designed for information exchange among highly mobile vehicles, the vehicle information collection in VANETs is made cheaper than that in cellular networks, with the adoption of the draft standard IEEE 802.11p [9] (DSRC).

[1]In this paper, the term V2V is used in two different contexts, namely, for communications among vehicles over VANETs and for energy swapping among GEVs, respectively.

This article has been accepted for publication in a future issue of this journal, but has not been fully edited. Content may change prior to final publication. Citation information: DOI 10.1109/TSG.2016.2593667, IEEE Transactions on Smart Grid

However, VANETs may suffer from intermittent disconnections due to the short-range V2V and V2R communications.

In this paper, cellular networks and VANETs are integrated into an heterogeneous wireless network to deliver messages for energy swapping. More efficient methods for message delivery can be deployed in the heterogeneous communication network that assumes low deployment and operation costs.

B. Transmission Mechanism in the Heterogeneous Wireless Network

Efficient GEV energy swapping strategies must be designed to consider real-time vehicle information (e.g., current locations, battery energy levels, drivers' behaviors, and charging abilities, etc.) in order to address the range anxiety problem and incorporate spatial coordination. To collect the information required by the energy swapping strategy in a real-time manner, cellular networks and VANETs are integrated into a heterogeneous wireless network (HetNet) to deliver messages.

Based on the heterogeneous wireless network, a GEV resorts first to the VANET for data transmission (either in V2V or V2R mode) when the connectivity probability in VANETs is estimated to be larger than a predefined threshold Γ, e.g., $\Gamma = 0.8$. The connectivity probability in VANETs can be estimated from the collected vehicle information and RSU deployment. As an example, the connectivity probability can be calculated based on vehicle density, vehicle mobility model, RSU deployment, etc [18]. The connectivity probability in VANETs can increase with 1) a surge in vehicle mobility parameters since an increased velocity reduces the average number of hops in a multihop VANET transmission link; 2) an expansion of vehicle density which may provide more opportunities to establish a successful V2V/V2R transmission; and 3) a rise in the transmission range and number of RSUs which provides more opportunities for V2R.

In the case that the estimated connectivity probability through VANETs is less than the threshold Γ, the GEV then relies on the cellular network for data transmission. Hence, the proposed architecture benefits from the VANET low transmission cost and relies on the cellular network only in case of poor V2V/V2R connections to guarantee successful information transmission. The proposed communication mechanism helps to relieve possible congestions induced by GEVs transmissions into the cellular network.

For analysis simplicity, in the link layer of VANETs, we consider an ideal medium access control (MAC) protocol. As one vehicle moves into the coverage area of an RSU, the RSU is able to schedule time slots for V2R transmission without collisions. In the proposed energy swapping strategy, the transmitted data packet size can be small. If the link data rate of a V2V or V2R transmission is considered to be constant, the contact duration between each transmission pair (e.g., V2V or V2R) is considered long enough to accomplish one packet delivery by appropriately setting the packet size.

C. Heterogeneous Wireless Network-Enhanced Smart Grid

Fig. 2 shows the proposed HetNet-enhanced smart grid architecture, consisting of a power distribution system, aggregators, RSUs, a base station (BS) of the cellular network, and

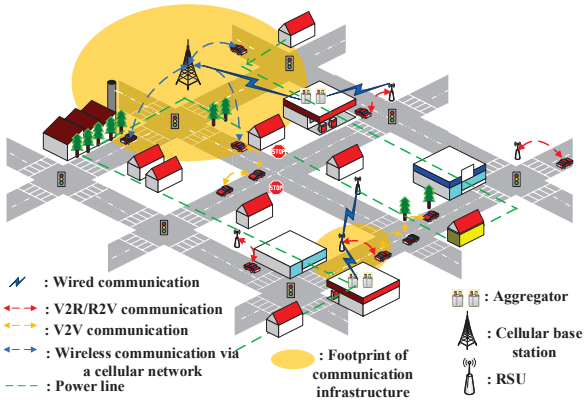

Fig. 2: HetNet-enhanced smart grid.

mobile GEVs. The power distribution system supplies energy to the whole network through power feeders/connection points (i.e., transmission lines). The set of connection points in the power grid is denoted as $\mathbb{B}$.

A set of aggregators is located in the network and connected to the power grid via transformers to a set of connection points $\mathbb{A}$ ($\mathbb{A} \subset \mathbb{B}$). The aggregators provide fast-charging/discharging for GEVs via V2V energy swapping [19]. Aggregators are controlled by the grid operator, to offload the heavy power demands. The aggregators are not only the infrastructure for charging/discharging but also the market organizer to make the price updates in our work. Time is partitioned into periods with equal duration τ. At the beginning of each period, through the remote terminal units (RTUs) readings, the maximal power that can be connected at aggregators is estimated in advance, i.e., the load/supply capacity of an aggregator which is denoted by C_a for the aggregator on connection point a (i.e., $B_a \in \mathbb{B}$). The aggregators manage the energy price u_k in period k for GEVs based on the load capacities, the collected GEV charging/discharging profiles (i.e., the maximum charging requests $\mathbb{P}_{\mathbb{D}}$ or discharging offers $\mathbb{P}_{\mathbb{S}}$), and their current locations.

RSUs are deployed along the roads, denoted as the set $\mathbb{R}$, to collect the GEV charging/discharging information (e.g., individual maximum charging requirements/discharging capabilities of GEVs and their current locations) through V2R transmissions in VANETs. A BS is also deployed in the network to support the cellular communications with portable transceivers in the GEVs. RSUs and the BS can relay the collected GEV information to aggregators based on wired connections, to determine the electricity price in order to balance energy demands and supplies. Thereafter, when the RSUs/BS receive the energy price from the aggregators, they relay the price to GEVs through the HetNet so that vehicles can make energy swapping decisions.

The set of mobile GEVs is denoted as $\mathbb{V}$. GEVs may need to be charged/discharged when moving along roads across the network. The set of GEVs that need to be charged is denoted by $\mathbb{D}$ ($\mathbb{D} \subset \mathbb{V}$) and is referred to as demanding GEVs, and the set of GEVs supplying electricity is $\mathbb{S}$ ($\mathbb{S} \subset \mathbb{V}$) and referred to supplying GEVs. The mobility of each GEV can be described by two random variables (M, N) [20], where M represents

This article has been accepted for publication in a future issue of this journal, but has not been fully edited. Content may change prior to final publication. Citation information: DOI 10.1109/TSG.2016.2593667, IEEE Transactions on Smart Grid

the GEV velocity which takes two possible state values (i.e., a lower velocity m_L and a higher velocity m_H), and $1/N$ stands for the transition rate between these two velocity states. Such a model can describe the realistic driving behaviors, e.g., a driver usually travels at one speed for a while and then changes to a higher/lower speed depending on his/her will and/or road conditions. Moreover, under this mobility model, vehicles are considered to move independently [21] and the headway distance[2] follows the exponential distribution with rate ζ [22] when the vehicle density is low or medium (e.g, no larger than 30 vehicle/km/lane).

The charging/discharging decisions of individual GEVs include the charging/discharging rate of GEV v at the aggregator on connection point a (i.e., B_a) in period k (denoted as $P_{v,a,k}$) and the charging/discharging indicator (denoted as $I_{v,a,k}$). If GEV v will be charged/discharged at the aggregator at connection point B_a in period k, $I_{v,a,k}$ is set to 1, otherwise it is set to 0. If GEV v is to be charged, the charging load $P_{v,a,k}$ is expressed as $P_{d,a,k}$ ($d \in \mathbb{D}$); otherwise, the discharging power $P_{v,a,k}$ is expressed as $P_{s,a,k}$ ($s \in \mathbb{S}$).

D. Power System Model

In general, the power system is composed of generation, transmission, distribution systems and customers. In this work, the aggregators are located in the distribution systems. As a case study, we consider a one-line diagram with multiple connection points (e.g., 12-connection point system) as a distribution system, as shown in Fig. 3, which can be extended directly to the larger system. To make the case study more appropriate, the considered 12-connection point system is connected to the feeder through a step down transformer. Transformers are in general highly efficient, and large power transformers (around 100 MVA and larger) may attain an efficiency as high as 99.75% [23]. In this work, the loss at transformer will not be considered in the problem formulation. Such an approximation has been applied in [24], [25].

Electricity price update is performed at the aggregators based on the collected GEV charging/discharging profiles and the load capacities of aggregators. There exist not only temporal fluctuations in the load capacity of each distribution feeder but also spatial fluctuations in the load capacities among different distribution feeders at the same time.

Fig. 3 shows the power system model as a one-line diagram with multiple connection points (e.g., 12-connection point system), which is abstracted from Fig. 2. The power system is supplied through the substation at the generation connection point. The set of aggregators $\mathbb{A}$ is located in the network at load connection points ($\in \mathbb{B}$), e.g., B_2 and B_{11}, respectively. Each aggregator is connected to the grid via a standard single-phase alternating-current (AC) connection [6]. The total charging demand (or discharging power) of GEVs at the aggregator on connection point B_a in period k is denoted as $P_D^{a,k}$ (or $P_S^{a,k}$). If the total discharging power cannot cover the total charging demand (i.e., $P_S^{a,k} < P_D^{a,k}$), the additional GEV power demand is drawed from the power grid at B_a in period

[2]In this paper, the headway distance is defined as the distance between two neighboring vehicles in the same lane.

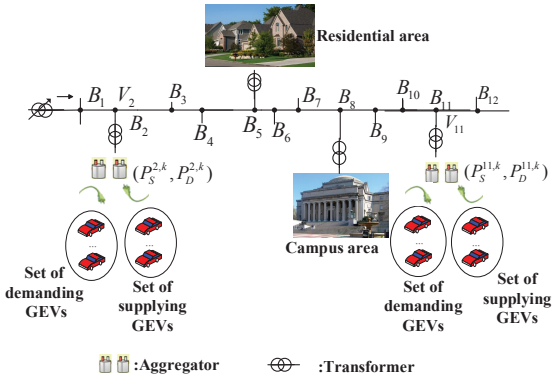

Fig. 3: Single line diagram of the system under study.

k, and is given by $P_L^{a,k} = P_D^{a,k} - P_S^{a,k}$, which is subject to a load-capacity constraint C_a due to the thermal limit of service cable or current rating of fuse [6]. On the other hand, when the total charging power is less than the possible discharging power, there is no additional load at this aggregator in the power grid, i.e., $P_L^{a,k} = 0$. Moreover, no additional power will be injected into the power grid.

The voltage drop between any two neighboring connection points, e.g., connection point i (e.g., B_1) and connection point j (e.g., B_2), in period k is $V_{i,k} - V_{j,k} = \frac{(P_{ij,k} - (P_D^{j,k} - P_S^{j,k})) \cdot r_{ij} + Q_{ij,k} \cdot x_{ij}}{V_{j,k}}$, $i, j \in \mathbb{B}$, where $V_{i,k}$ and $V_{j,k}$ are the voltages at B_i and B_j in period k; $P_{ij,k}$ and $Q_{ij,k}$ are the active and reactive power flows from B_i to B_j in period k, respectively [26]. As aforementioned, $P_D^{j,k} - P_S^{j,k}$ represents the power load added to connection point j. Here, r_{ij} and x_{ij} are the real and imaginary part of the impedance of the feeder line i-j [26]. Per unit, the power flow equation can be approximated as:

$$V_{i,k} - V_{j,k} = (P_{ij,k} - P_L^{j,k}) \cdot r_{ij} + Q_{ij,k} \cdot x_{ij}. \quad (1)$$

Since all the voltages of the connection points should be within a certain range [26], the voltage magnitude at B_j in period k is bounded by both lower and upper limits, $V_{j,k}^{\min}$ and $V_{j,k}^{\max}$, respectively, i.e., $V_{j,k}^{\min} \le V_{j,k} \le V_{j,k}^{\max}$. Thus, based on the power flow equation (1) and the voltage limits, the total power supply from the power grid to a GEV aggregator a in period k at connection point a, i.e., $P_L^{a,k}$, can be calculated and bounded by the load capacity of the feeder in period k, C_a^k [6],

$$P_L^{a,k} \le P_{ia,k} - \frac{V_{i,k} - V_{\max} - Q_{ia,k} \cdot x_{ia}}{r_{ia}} = C_a^k \quad (2)$$

where $V_{i,k}$, $P_{ia,k}$, and $Q_{ia,k}$ can be found from RTU readings.

E. GEV Charging/Discharging Models

For a mobile demanding (or supplying) GEV, the charging load of GEV d ($\in \mathbb{D}$) (or discharging power of GEV s ($\in \mathbb{S}$)) at aggregator a ($\in \mathbb{A}$) in period k, i.e., $P_{d,a,k}$ (or $P_{s,a,k}$), should be within a certain range due to the GEV charger output (input) power constraint [28], i.e.,

$$0 \le P_{d,a,k} \le P_{d,a,k}^{\max} \text{ and } 0 \le P_{s,a,k} \le P_{s,a,k}^{\max} \quad (3)$$

This article has been accepted for publication in a future issue of this journal, but has not been fully edited. Content may change prior to final publication. Citation information: DOI 10.1109/TSG.2016.2593667, IEEE Transactions on Smart Grid

where $P_{d,a,k}^{\max}$ (or $P_{s,a,k}^{\max}$) is the upper bound of the charging load $P_{d,a,k}$ (or discharging power $P_{s,a,k}$). If GEV d (or s) does not plan to get charged (or discharged) at aggregator a in period k, i.e., $I_{d,a,k}=0$ (or $I_{s,a,k}=0$), the charging load of GEV d (or discharging power of GEV s) at aggregator a in period k is 0,

$$\frac{P_{d,a,k}}{P_{d,a,k}^{\max}} \leq I_{d,a,k} \text{ and } \frac{P_{s,a,k}}{P_{s,a,k}^{\max}} \leq I_{s,a,k}. \tag{4}$$

A GEV can be dispatched to at most one aggregator in one period. Charging (discharging) indicator $I_{d,a,k}(I_{s,a,k})$ satisfies

$$\sum_{a\in\mathbb{A}} I_{d,a,k} \leq 1 \text{ and } \sum_{a\in\mathbb{A}} I_{s,a,k} \leq 1;\ I_{d,a,k}, I_{s,a,k} \in I=[0,1]\cap\mathbb{Z} \tag{5}$$

where $\mathbb{Z}$ is the integer set. And

$$\sum_{k}\sum_{a\in\mathbb{A}} I_{d,a,k} \leq I_D^{\max} \text{ and } \sum_{k}\sum_{a\in\mathbb{A}} I_{s,a,k} \leq I_S^{\max}, \tag{6}$$

where $I_D^{\max}$(or $I_S^{\max}$) is the upper bound of the total charging (or discharging) times for a demand (or supply) GEV within all the considered periods, since frequent charging (or discharging) may result in GEV battery damage [27]. Then, the total charging load (or discharging power) of demanding (or supplying) GEVs $P_D^{a,k}$(or $P_S^{a,k}$) at aggregator a in period k is $P_D^{a,k}=\sum_{d\in\mathbb{D}} P_{d,a,k}$ (or $P_S^{a,k}=\sum_{s\in\mathbb{S}} P_{s,a,k}$). The total charging demand (or discharging power) of the whole network in period k is $P_D^k=\sum_{a\in\mathbb{A}} P_D^{a,k}$ (or $P_S^k=\sum_{a\in\mathbb{A}} P_S^{a,k}$).

F. Electricity Price Model

As shown in Fig. 4, based on the collected GEV profiles (e.g., charging requirements $\mathbb{P}_{\mathbb{D}}$ and discharging capabilities $\mathbb{P}_{\mathbb{S}}$) by the HetNet, aggregators specify the electricity price. Two cases can be distinguished for price decision:

- High demand case: If the collected $\mathbb{P}_{\mathbb{D}}$ is larger than $\mathbb{P}_{\mathbb{S}}$ in period k, the electricity price in period k, i.e., $u_k{}'$, is determined based on the amount of GEV energy supply (i.e., P_S^k), $u_k{}'=b_1-b_2P_S^k$, where b_1 and b_2 are the positive coefficients of the linear price function [11]. The supplying GEVs sell energy at price $u_k{}'$. In this case, some GEVs with charging demands may be turned down by V2V charging. Then, these GEVs may be served by the power grid via G2V charging, following the current electricity price in the power grid, e.g., $u_k{}''$. Hence, eventually, supply and demand matching is satisfied at the aggregator. The final electricity price announced to the demand side is the average price u_k over both supply parts (i.e., the supplying GEVs and the power grid), i.e., $u_k=\frac{P_S^k}{\mathbb{P}_{\mathbb{D}}}\cdot u_k{}'+\frac{\mathbb{P}_{\mathbb{D}}-P_S^k}{\mathbb{P}_{\mathbb{D}}}\cdot u_k{}''$.
- Surplus supply case: If $\mathbb{P}_{\mathbb{S}}$ is no less than $\mathbb{P}_{\mathbb{D}}$ in period k, the electricity price is determined based on GEV demands P_D^k in period k. The energy price on the demand side is $u_k=b_1-b_2P_D^k$, and the energy price on the supply side $u_k{}'$ is equal to u_k. In this case, some GEVs with discharging capabilities may not be involved in the V2V transaction, and eventually the supply and demand matching is satisfied at the aggregator.

Once the aggregator has determined the electricity price, a price control signal is delivered to GEVs via the HetNet. Based on the received electricity price, GEVs will make their charging/discharging decisions. Note that as shown in [11], a linear price function among many possible price functions can not only reveal the market competing philosophy but also take advantage of the symmetry of the model. In addition, by this linear function, the equilibrium does converge to a competitive equilibrium. The parameter in the linear function (i.e., b_1 and b_2 in our manuscript) should be decided or calculated by the market operator based on the market situation, for instance, the grid operator.

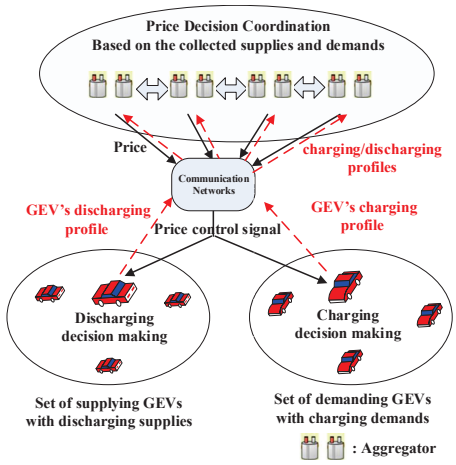

Fig. 4: Illustration of spatio-temporal coordinated V2V energy swapping strategy based on price control.

G. Overview on Proposed Energy Swapping Strategy

Efficient spatial coordination of mobile GEVs charging/discharging should account for the GEVs range anxieties, otherwise, the batteries of demanding GEVs will be depleted on their way to the aggregator and less revenues will be achieved for the supplying GEVs. Hence, efficient GEV energy swapping strategies must be designed to consider real-time vehicle information (e.g., current locations and battery energy levels) in order to address the range anxiety problem and incorporate spatial coordination.

In summary, the proposed energy swapping strategy operates based on the information exchange in two stages, as shown in Fig. 4:

- Price update at the aggregators: To balance the power demands and power supplies at the aggregators, the electricity price is updated based on the collected information, which includes the historic remote terminal unit (RTU) readings of the connection points at aggregators in the power system and potential GEV charging/discharging requests/offers. The RTU readings are gathered by the aggregators through a wired connection, based on which the charging load capacity constraints at the aggregators can be estimated. The GEVs' energy requests/offers are collected from the vehicles via the heterogeneous wireless network, based on which GEVs' energy demand/supply conditions can be estimated. Aggregators communicate with each other via the wired connections to exchange information regarding the total power demands and power supplies to determine the electricity price.

This article has been accepted for publication in a future issue of this journal, but has not been fully edited. Content may change prior to final publication. Citation information: DOI 10.1109/TSG.2016.2593667, IEEE Transactions on Smart Grid

- Coordinated GEV charging/discharging decision making: The aggregators broadcast the updated electricity price to the GEVs, based on which the GEVs calculate the optimal GEV charging/discharging decisions by considering the range anxieties and the charging cost or discharging revenues. The GEV charging/discharging decisions include both the charging/discharging rate for vehicle v at aggregator a in period k, $P_{v,a,k}$, and the charging/discharging indicator, $I_{v,a,k}$, which equals 1 if vehicle v is scheduled to charge/discharge at aggregator a in period k, and equals 0 otherwise. The decisions are in turn sent back to aggregators.

Once a charging/discharging decision is made, the decision is available to the GEV global positioning system (GPS) device, which will navigate the GEV to the assigned aggregator.

Here, the primary objective of the proposed V2V energy swapping strategy is to prevent the grid from overloading rather than to minimize the charging cost for demanding GEVs first. Consider that at peak-demand time and when considering the high demand case, neither V2V nor the power grid alone can satisfy the target demand. In that sense, some GEVs rely on V2V to get charged and the rest rely on the grid limited capability at peak-load to satisfy its demand (if possible). On the other hand, when considering the surplus supply case and since the grid is again assumed to be at peak-demand time, V2V alone can support all target demands and completely offload this demand from the power grid.

Note that since it is not very possible to add additional infrastructure or power lines in the power system to connect the aggregators directly, aggregators are usually connected to the existing distributed systems. Even assuming supplying GEV has V2G capability, it cannot be guaranteed that all the injected energy from V2G at one connection point (e.g., at B_2 in Fig. 3) can be utilized by the particular connection point (e.g., the aggregator at B_{11} in Fig. 3), and thus the total amount of charged energy by demanding GEVs may be reduced compared to that through V2V energy swapping.

IV. Problem Formulation

In this section, the power balance constraint, GEV charging/discharging constraints, and travel costs of GEVs are explained. Finally, optimization problems are discussed.

A. Power balance constraint at the aggregator

For V2V energy swapping at the aggregators, the total charging power is balanced with the total discharging power:

$$\sum_{s\in\mathbb{S}} P_{s,a,k} + P_L^{a,k} = \sum_{d\in\mathbb{D}} P_{d,a,k}, \forall a \in \mathbb{A}. \tag{7}$$

For the high demand case, since the supplied energy from supplying GEVs cannot satisfy all demanded energy, electric energy has to be drawn from the power grid. For the surplus supply case, no extra energy is required from the power grid, i.e., $P_L^{a,k} = 0$.

B. GEV Charging/Discharging Constraints

The charging (or discharging) energy of each GEV should be limited by its battery-capacity E, and the battery should not be depleted on the way to the aggregator, i.e.,

$$\begin{aligned} &0 \le E_{d,k}^{init} + (\sum_{a\in\mathbb{A}} \Delta P_{d,a,k} - E_{cost}^{d,k} - E_{cons}^{k}(1 - \sum_{a\in\mathbb{A}} I_{d,a,k})) \le E, \\ &\text{and} \\ &E_s \le E_{s,k}^{init} + (-\sum_{a\in\mathbb{A}} \Delta P_{s,a,k} - E_{cost}^{s,k} - E_{cons}^{k}(1 - \sum_{a\in\mathbb{A}} I_{s,a,k})) \le E, \end{aligned} \tag{8}$$

where $E_{d,k}^{init}$ (or $E_{s,k}^{init}$) is the initial energy stored in GEV d (or GEV s) in period k, and $E_{cost}^{d,k}$ (or $E_{cost}^{s,k}$) is the travel cost for charging (or discharging) in period k for GEV d (or GEV s) routing to aggregator a (see next subsection). Let E_{cons}^{k} be the average energy cost of each GEV to keep moving on the road if the GEV is not charged (or discharged) in period k. The energy swapping duration in each period is set to Δ hours. For instance, if we consider a 30-minute energy swapping duration for each period, $\Delta = 0.5$. Without loss of generality, consider this charging (or discharging) duration to be the same for all demanding (or supplying) GEVs. In addition, after discharging, GEV s should keep a minimum amount of energy E_s at its battery to guarantee the expected energy required to complete its own journey, after period k.

Hence, the charging (or discharging) cost $c_{d,k}$ (or $c_{s,k}$) for GEV d (or GEV s) with charging (or discharging) power $\sum_{a\in\mathbb{A}} \Delta \cdot P_{d,a,k}$ (or $\sum_{a\in\mathbb{A}} \Delta \cdot P_{s,a,k}$) in period k is

$$\begin{aligned} &c_{d,k} = u_k \cdot \sum_{a\in\mathbb{A}} \Delta \cdot P_{d,a,k} + u_d \cdot E_{cost}^{d,k} + W_d + \mathfrak{T}_{d,k} \\ &\text{and } c_{s,k} = u_s \cdot (\sum_{a\in\mathbb{A}} \Delta \cdot P_{s,a,k} + E_{cost}^{s,k}) + W_s + \mathfrak{T}_{s,k}, \end{aligned} \tag{9}$$

where u_k is the energy price in period k, as set by the aggregator. Let u_s (u_d) denote the preknown price at which GEV s (GEV d) purchased its stored energy originally. The quadratic battery wear cost function of charging GEV d [28] is defined as $W_d = e_1(\sum_{w\in W} \Delta \cdot P_{d,a,k})^2 + e_2(\sum_{a\in\mathbb{A}} \Delta \cdot P_{d,a,k}) + e_3$, where e_1, e_2, and e_3 are the coefficients of the function with $e_1, e_2, e_3 \ge 0$. The quadratic battery wear cost function for discharging GEV s can be determined to be W_s in the same way as W_d. Based on the designed communication mechanism, $\mathfrak{T}_{d,k}$ (or $\mathfrak{T}_{s,k}$) is the monetary cost of information transmission for GEV d (or GEV s) in period k. When GEVs use cellular networks to deliver the message, drivers have to pay transmission fees; otherwise, $\mathfrak{T}_{d,k} = 0$ (or $\mathfrak{T}_{s,k} = 0$) for VANETs. Then, the revenue $R_{s,k}$ of the supplied GEV s is

$$R_{s,k} = u_k{}' \cdot \sum_{a\in\mathbb{A}} \Delta \cdot P_{s,a,k} - c_{s,k}, \tag{10}$$

where $u_k{}'$ is the energy selling price for supplied GEVs.

C. Travel Cost for GEVs and Range Anxiety

If the V2V strategy guides GEV v to be charged/discharged in the next period k, then $\sum_{a\in\mathbb{A}} I_{v,a,k} = 1$. The travel time spent on highways and local roads by GEV v from its current position to an aggregator in period k is denoted as $t_{v,k}^{hy}$ and $t_{v,k}^{lc}$, respectively. The travel time is affected by many factors, including drivers' behaviors (e.g., the driver prefers highways/local roads, or avoids certain road segments, etc.), working hours (rush hours may lead to traffic jam), and traffic conditions (e.g., road gridlock and traffic congestion). Using the GPS device, travel time could be estimated by combining the preferred path information and the real-time

This article has been accepted for publication in a future issue of this journal, but has not been fully edited. Content may change prior to final publication. Citation information: DOI 10.1109/TSG.2016.2593667, IEEE Transactions on Smart Grid

traffic conditions collected from the heterogeneous network [29]. Thus, the travel time of GEV v in period k for charging is defined as $t^{hy}_{v,k} + t^{lc}_{v,k} = \sum_{a\in\mathbb{A}} [t^{hy}(I_{v,a,k}) + t^{lc}(I_{v,a,k})]\cdot I_{v,a,k}$, where $t^{hy}(I_{v,a,k})$ ($t^{lc}(I_{v,a,k})$) denotes the actual time spent on highway (local roads) if GEV v is scheduled to aggregator a. Based on $t^{hy}_{v,k}$ and $t^{lc}_{v,k}$, we denote $F(t^{hy}_{v,k}, t^{lc}_{v,k})$ as the travel cost for GEV v in period k in terms of energy, where $F(\cdot)$ is a linear non-decreasing function to measure the impact of travel time on the travel cost [5]. The coefficients of the linear function can be achieved based on statistics of the vehicle fuel economics for highways and local roads, respectively. Due to the range anxiety, the current stored energy $E^{init}_{v,k}$ is no less than $F(t^{hy}_{v,k}, t^{lc}_{v,k})$; otherwise, the battery will be depleted before the GEV reaches the destination, i.e.,

$$E^{v,k}_{cost} = F(t^{hy}_{v,k}, t^{lc}_{v,k}) \leq E^{init}_{v,k}. \tag{11}$$

In our simulation, we consider a suburban scenario without highways and use shortest path algorithm [29] and constant traffic density in measuring the GEV range anxiety as a case study. In addition, for demanding GEVs, the travel cost should be no less than the charging energy, i.e.,

$$E^{d,k}_{cost} \leq \Delta \times P_{d,a,k}. \tag{12}$$

D. V2V Charging/Discharging Optimization Problems

Considering GEV discharging capabilities, charging demands and energy price, our strategy is modeled as a time-coupled Oligopoly game [11] and an MINLP in two cases:

- High Demand Case: When $\mathbb{P}_{\mathbb{S}}$ is less than $\mathbb{P}_{\mathbb{D}}$, the problem is solved in two steps. The first one is the *price decision making step* where the electricity price is determined based on the supply side, P^k_S. The supplying GEVs compete for energy discharge based on an Oligopoly game, to maximize the discharging revenues as

$$\begin{aligned} &\max_{P_{s,a,k}, I_{s,a,k}} \sum_k R_{s,k},\ \forall s \in \mathbb{S} \\ &s.t., (3)-(6), (8), (11). \end{aligned} \tag{13}$$

Thereafter, the optimal price ${u_k}'^*$ can be considered into the total energy supplied from GEVs as $P^*_{s,k} = \frac{b_1}{b_2} - \frac{{u_k}'^*}{b_2}$. The second step is the *charging decision making step*, based on the specified price $u^*_k = \frac{P^k_S}{\mathbb{P}_{\mathbb{D}}} \times {u_k}'^* + \frac{\mathbb{P}_{\mathbb{D}} - P^k_S}{\mathbb{P}_{\mathbb{D}}} \times u_k{}''$ where ${u_k}'^*$ is the solution of (13) and $u_k{}''$ is the energy price of the power grid in period k. GEVs with discharging demands aim to minimize total charging cost

$$\begin{aligned} &\min_{P_{d,a,k}, I_{d,a,k}} \sum_k \sum_{d\in\mathbb{D}} c_{d,k} \\ &s.t., (2)-(6), (7), (8), (11), (12). \end{aligned} \tag{14}$$

- Surplus Supply Case: When $\mathbb{P}_{\mathbb{S}}$ is no less than $\mathbb{P}_{\mathbb{D}}$, the electricity price is determined based on the demand side, P^k_D. *In the price decision making step*, GEVs with charging demands compete for energy charging based on a time-coupled Oligopoly game to minimize charging costs

$$\begin{aligned} &\min_{P_{d,a,k}, I_{d,a,k}} \sum_k c_{d,k},\ \forall d \in \mathbb{D} \\ &s.t., (3)-(6), (8), (11), (12). \end{aligned} \tag{15}$$

The optimal price u^*_k can be obtained from the total demanded energy by GEVs as $P^*_{d,k} = \frac{b_1}{b_2} - \frac{u^*_k}{b_2}$.
In the discharging decision making step, based on the specified price, the GEVs with discharging supply aim to maximize revenues, i.e.,

$$\begin{aligned} &\max_{P_{s,a,k}, I_{s,a,k}} \sum_k \sum_{s\in\mathbb{S}} R_{s,k} \\ &s.t., (3)-(6), (7), (8), (11). \end{aligned} \tag{16}$$

V2V energy swapping relieves the peak-demand of GEV charging in two folds. First, V2V energy swapping offloads the peak charging demand from the grid to the aggregators and exploits the excessive GEV energy to match the charging demand. Second, when the total available energy from both grid and supplying GEVs is still not enough to match the peak charging demand (in extremely high demand case), to prevent the grid from overloading, optimization problem (14) determines: i) the optimal charging period (i.e., temporal coordination) and rate for each demanding GEV to guarantee that the load capacity constraints are not violated, and ii) the optimal charging aggregator (i.e., spatial coordination) while considering the GEV range anxiety and distributing the demanding GEVs among all the aggregators as much as possible. In this manner, the peak-hour load is shifted and the spatial demand relocation is achieved.

Note that Equation (13) is the optimization problem of each individual supply GEV to maximize its own revenues during the Oligopoly Game. The Oligopoly Game is proven in our work to have a Nash equilibrium that can maximize the individual revenue for each supplying GEV. Even if a supplying GEV discharge more energy than the amount given in the equilibrium, it may get less revenue, which can be evaluated in the simulation parts.

V. Online Spatio-Temporal Coordinated V2V Charging/Discharging Strategy

In this section, we derive the solutions of (13)-(16) to design the coordinated V2V energy swapping strategy. We only present the detailed methodology for the solution in the high demand case as an example, and due to space limitations we omit the mathematical details for the surplus supply case, which follows the same procedure as the high demand case.

A. Price Decision Making in High Demand Case

Due to the objective function, the original problem (13) is a time-coupled MINLP problem w.r.t period k, thus being very complicated to solve. However, as the only time-coupled constraint, i.e., $\sum_k \sum_{a\in\mathbb{A}} I_{s,a,k} \leq I^{\max}_S$, $\forall s \in \mathbb{S}$, is linear, the original time-coupled MINLP problem (13) can be first time-decoupled into a series of sub-MINLPs through Lagrange duality [12], $L(P_{s,a,k}, I_{s,a,k}) = \sum_k R_{s,k} - \lambda_s[\sum_k \sum_{a\in\mathbb{A}} I_{s,a,k} - I^{\max}_S]$, where $\lambda_s \geq 0$ is Lagrange multiplier associated with the sth inequality constraint $\sum_k \sum_{a\in\mathbb{A}} I_{s,a,k} \leq I^{\max}_S$. Define $D^k(\lambda_s)$ as

$$D^k(\lambda_s) = \max_{P_{s,a,k}, I_{s,a,k}} \{R_{s,k} - \sum_{a\in\mathbb{A}} \lambda_s I_{s,a,k}\}. \tag{17}$$

Let the Lagrangian dual function $D(\lambda_s)$ be the maximum of the Lagrangian function $L(\cdot)$ over all $P_{s,a,k}$ and $I_{s,a,k}$, we have $D(\lambda_s) = \sum_k D^k(\lambda_s) + \lambda_s I^{\max}_S$. By minimizing the Lagrangian dual function over all dual variables λ_s, the ϵ-optimal solution of the original problem (13) can be obtained,

This article has been accepted for publication in a future issue of this journal, but has not been fully edited. Content may change prior to final publication. Citation information: DOI 10.1109/TSG.2016.2593667, IEEE Transactions on Smart Grid

$$\min_{\lambda_s,\ s\in\mathbb{S}} D(\lambda_s) \quad s.t.\ \lambda_s \geq 0. \tag{18}$$

As shown in [30], given λ_s, if the optimal solution $\{P_{s,a,k}\}$ and $\{I_{s,a,k}\}$ of (17) satisfies the time-coupled constraint, the solution is ϵ-optimal to the original problem, with $\epsilon = -\lambda_s(\sum_k \sum_{a\in\mathbb{A}} I_{s,a,k} - I_S^{\max})$. Each sub-MINLP (17) corresponds to a period k with only parameters and decision variables corresponding to that period. In the *price decision making step*, in Theorem 1, we show that for a supplying GEV, if the Nash equilibrium exists, the aggregator assigned to each discharging GEV is the nearest one for this GEV; that is, the integer variable $I_{s,a,k}$ can be determined apriori.

Theorem 1: (**The nearest, the best**) In the high demand case, the aggregator assigned for each supplying GEV is the nearest one.

Proof: See the Appendix. ∎

Hence, the sub-MINLP (17) becomes an Oligopoly game among GEVs with only the continuous decision variable, $P_{s,a,k}$, and can be solved as discussed in [11]. Furthermore, similar to [11], the optimal selling price ${u_k}'^*$ can be found as the global revenue-maximum for each GEV [11].

B. Charging Decision Making in High Demand Case

Given the optimal selling price ${u_k}'^*$ for the supplying GEVs, the energy buying price for demanding GEVs (i.e., u_k^*) is given by $u_k^* = \frac{P_S^k}{\mathbb{P}_\mathbb{D}} \cdot {u_k}'^* + \frac{\mathbb{P}_\mathbb{D} - P_S^k}{\mathbb{P}_\mathbb{D}} \cdot {u_k}''$. In order to minimize the charging costs for GEVs, we solve (14) which presents a convex objective function with all linear constraints. Using the Lagrange duality theory [12], we can decouple problem (14). The decoupling procedure is very similar to that in solving problem (13). Thus, we directly present the decoupled sub-optimization problem (with the Lagrange multiplier λ_d) w.r.t period k in the following, which is denoted as problem $\mathcal{P}$.

$$\mathcal{P}\begin{cases} \min\limits_{P_{d,a,k}, I_{d,a,k}} \sum\limits_{d\in\mathbb{D}} c_{d,k} + \sum\limits_{d\in\mathbb{D}} \sum\limits_{a\in\mathbb{A}} \lambda_d I_{d,a,k} \\ s.t. \\ f_{d,a,1}(I_k,P_k) = \frac{P_{d,a,k}}{P_{d,a,k}^{\max}} - I_{d,a,k} \leq 0, \forall d\in\mathbb{D}, \forall a\in\mathbb{A} \\ f_{d,2}(I_k,P_k) = \sum\limits_{a\in\mathbb{A}} I_{d,a,k} - 1 \leq 0, \forall d\in\mathbb{D} \\ f_{a,3}(I_k,P_k) = \sum\limits_{s\in\mathbb{S}} P_{s,a,k} + P_L^{a,k} - \sum\limits_{d\in\mathbb{D}} P_{d,a,k} \leq 0, \forall a\in\mathbb{A} \\ f_{a,4}(I_k,P_k) = \sum\limits_{d\in\mathbb{D}} P_{d,a,k} - \sum\limits_{s\in\mathbb{S}} P_{s,a,k} - P_L^{a,k} \leq 0, \forall a\in\mathbb{A} \\ f_{a,5}(I_k,P_k) = P_L^{a,k} - P_{ia,k} + \frac{V_{i,k}-V_{\max}}{r_{ia}} \leq 0,\ \forall i\in\mathbb{B},\ a\in\mathbb{A} \\ f_{d,6}(I_k,P_k) = E_{d,k}^{init} + (\sum\limits_{a\in\mathbb{A}} \Delta\cdot P_{d,a,k} - F(t_{d,k}^{hy}, t_{d,k}^{lc}) \\ \qquad -E_{cons}^k(1-\sum\limits_a I_{d,a,k})) - E \leq 0, \forall d\in\mathbb{D} \\ f_{d,7}(I_k,P_k) = -[E_{d,k}^{init} + (\sum\limits_{a\in\mathbb{A}} \Delta\cdot P_{d,a,k} - F(t_{d,k}^{hy}, t_{d,k}^{lc}) \\ \qquad -E_{cons}^k(1-\sum\limits_a I_{d,a,k}))] \leq 0, \forall d\in\mathbb{D} \\ f_{d,8}(I_k,P_k) = F(t_{d,k}^{hy}, t_{d,k}^{lc}) - E_{d,k}^{init} \leq 0, \forall d\in\mathbb{D} \\ f_{d,a,9}(I_k,P_k) = F(t_{d,k}^{hy}, t_{d,k}^{lc}) - \Delta P_{d,a,k} \leq 0, \forall d\in\mathbb{D},\ \forall a\in\mathbb{A} \\ 0 \leq P_{d,a,k} \leq P_{d,a,k}^{\max},\ \ I_{d,a,k}\in\{0,1\},\ \ \forall d\in\mathbb{D} \end{cases} \tag{19}$$

where I_k and P_k are the set of $\{I_{d,a,k}\}$ and $\{P_{d,a,k}\}$ $(\forall d, a)$ in period k, respectively. Since the sub-optimization problem (19) is an MINLP as it involves both binary and continuous decision variables, it can be solved by the BCBOA algorithm [13]. The BCBOA algorithm is an iterative procedure that solves the original MINLP by solving an alternating sequence of relaxed (mixed-integer linear program) MILPs and nonlinear programs (NLPs). The relaxed MILP is obtained from the original problem $\mathcal{P}$ by replacing the original constraints of linear functions by polyhedral outer approximations (OAs). The OA is to provide a polyhedral representation of the feasible space $\mathcal{P}$. Such a representation hence reduces the complexity of the original problem. Given any set of feasible solutions for problem $\mathcal{P}$, e.g., $\mathbb{T} = \{(I_k^1, P_k^1), ..., (I_k^t, P^t)_k, ...\}$, the MINLP (19) is relaxed to the MILP as

$$\mathcal{P}^{OA}(\mathbb{T})\begin{cases} \max\limits_{P_{d,a,k}, I_{d,a,k}} \varpi \\ s.t. \\ \nabla G(I_k,P_k)^T_{|(I_k^t,P_k^t)} \begin{pmatrix} I_k - I_k^t \\ P_k - P_k^t \end{pmatrix} + G(I_k^t, P^t{}_k) \geq \varpi \\ \nabla \mathfrak{F}(I_k,P_k)^T_{|(I_k^t,P_k^t)} \begin{pmatrix} I_k - I_k^t \\ P_k - P_k^t \end{pmatrix} + \mathfrak{F}(I_k^t, P_k^t) \leq 0 \\ \forall (I_k^t, P_k^t)\in\mathbb{T},\ I_k \cap \mathbb{Z}^n, \\ 0 \leq P_{d,a,k} \leq P_{d,a,k}^{\max}, \end{cases} \tag{20}$$

where $G(I_k,P_k) = \sum\limits_{d\in\mathbb{D}} c_{d,k} + \sum\limits_{d\in\mathbb{D}} \sum\limits_{a\in\mathbb{A}} \lambda_d I_{d,a,k}$, $\mathfrak{F} = \{f_{d,a,1}, f_{d,2}, f_{a,3}, f_{a,4}, f_{a,5}, f_{d,6}, f_{d,7}, f_{d,8}, f_{d,a,9}\}$ $(\forall d \in \mathbb{D},\ \forall a\in\mathbb{A})$, ϖ is an auxiliary variable, and $\nabla G(\cdot)^T$ denotes the transpose of the gradient of G. According to Theorem 1 in [31], if $\mathbb{T}$ contains suitable points and the KKT conditions are satisfied at these points, the relaxed MILP is equivalent to the MINLP (19). $\mathbb{T}$ is calculated from the branch-and-cut involved in the BCBOA algorithm. Theorem 1 in [31] shows that if 1) the solution set, $\mathbb{T}$, contains suitable solutions of the original problem; 2) KKT conditions are satisfied at these points, then the problems $\mathcal{P}^{OA}(\mathbb{T})$ and $\mathcal{P}$ are equivalent.

The proposed charging strategy can be obtained by first time-decoupling the original problem into a series of sub-MINLPs through Lagrange duality (19). With BCBOA algorithm, each sub-MINLP is broken into an alternating sequence of MILPs and NLPs. Each MILP can be solved via the branch-and-cut method. Each NLP can be solved by convex optimization techniques, since the objective function is convex and all constraints are linear. The optimal solution leads to the charging decisions, i.e., $P_{d,a,k}$ and $I_{d,a,k}$. These decisions are dispatched to GEVs by heterogeneous networks.

Remark 1: In the high demand case, if a given charging power with a farther aggregator is feasible, the same charging power may not be feasible for a nearer aggregator due to the aggregator charging capacity constraint. Thus, the nearest aggregator is not always the best choice for demanding GEVs for charging decision making, leading to the essentiality of the spatial coordinations between demanding GEVs and aggregators.

Remark 2: For the surplus supply case, the nearest charging place is always the best for demanding GEVs, while the nearest aggregator is not always the best choice for supplying GEVs due to the supply capacity of the individual aggregator, leading to the essentiality of the spatial coordinations between supplying GEVs and aggregators.

Remark 3: As V2V energy swapping is conducted at the aggregator, energy can be directly and locally transferred among GEVs instead of bi-directional V2G/G2V operations, thus significantly reducing the involvement level of the smart grid and the implementation complexity. Besides, the downside of the V2V energy swapping strategy is the additional but simple infrastructure requirements on the aggregators.

This article has been accepted for publication in a future issue of this journal, but has not been fully edited. Content may change prior to final publication. Citation information: DOI 10.1109/TSG.2016.2593667, IEEE Transactions on Smart Grid

VI. Performance Evaluation

A. Simulation Setup

A realistic suburban scenario that represents the region around the campus of University of Waterloo (Waterloo, ON, Canada) is considered in the simulation environment, as shown in Fig. 5. RSUs are uniformly deployed along the roads, and two aggregators are deployed in Fig. 5(a). The parameters of the 12-connection point distribution system (only load points) in [26] are considered with the load enlarged to the MW level. Two aggregators are connected to connection points B_2 and B_{11}, respectively. The loads connected to each connection point at 21:00 is given in Table I. The input voltage is set to 1.0 per unit (pu), and the minimum allowable voltage is 0.9 pu, with the impedance of any line section being $r = 0.005$ and $x = 0.0046$. The normalized power over the power at 21:00 for all the connection points without GEV charging load is shown in Table II, according to the trend in [32]. The load values at the aggregators are to be determined (TBD), as indicated in Table I. In this section, we first consider the high demand case to evaluate the strategy performance, and due to space limitations we briefly explain the performance under the surplus supply case.

In addition, vehicles on the road follow the mobility model in Section III-C. To model the vehicle traffic, a highly-realistic microscopic vehicle traffic simulator, VISSIM [14], is employed to generate vehicle trace files to record vehicle mobility characteristics. Based on the trace files and power system data, we evaluate the performance of the proposed energy swapping strategy by a custom simulator built in Matlab.

1) VISSIM Setup: To simulate a vehicular network with VISSIM, vehicles are distributed in a region of 6000 m $\times$ 2800 m, as shown in Fig. 5(a). At the beginning of the simulation, vehicles enter the region following a Poisson process at rate ζ (e.g., ζ = 2500 vehicle/hour/entry) from the preseted entries. After a certain duration t_ζ (e.g., 240 sec), the vehicles stop entering the region. The car following model, Wiedemann 74 model [33], is utilized to model the traffic. The velocity distribution for all vehicles follows the velocity model described in Subsection III-C with parameters $M = \{m_L, m_H\}$ and N (e.g., taking $m_L = 30$ km/hour, $m_H = 60$ km/hour, $N = 60$ s as a case study). The information (e.g., locations, velocities, etc.) of vehicles is recorded at the end of every simulation step (e.g., 0.2 sec) in the recorded trace files. We consider two groups of vehicles, i.e., supply group and demand group. For each group, the GEV penetration level of the group of vehicles is set at 10%. For example, in the supply group with 600 vehicles, only 60 vehicles of them are GEVs and can contribute in a V2V energy swapping transaction. In addition, 25 RSUs are deployed uniformly along roads in the region, with transmission range of 150 m. The coverage range of a BS is set to 1500 m. The total simulation time is 3000 sec.

2) Energy Swapping Setup: In the V2V strategy evaluations, we set the GEV battery capacity to 85 KWh according to the TESLA Model S [1]. The energy swapping period is set to 30 min as a case study, with a maximum charging energy of 30 KWh. If a GEV is not scheduled for charging/discharging in a period, the energy cost for running on the road in that period is uniformly chosen within [0, 10] KWh. The coefficients of the linear price function, i.e., b_1 and b_2, are set to 40 and 0.004, respectively. The initial state of remaining energy in the battery for each GEV is uniformly chosen from [20, 50] KWh. The ending state of remaining energy in the battery for each supplying GEV (i.e., E_s) is set to 10 KWh.

To better illustrate the performance of the proposed V2V energy swapping strategy, the centralized charging strategy in [6] is used as as benchmark where the optimization objective is to only maximize the total amount of GEV charging energy without considering the mobility of GEVs or spatial coordinations. The performance evaluation metrics include the total amount of demanded energy (TADE), the number of GEVs successfully charged, and the average charging cost.

B. Evaluation of Data Transmissions in the Heterogeneous Wireless Network

Based on the trace files from VISSIM, Fig. 6 shows the probability density function (PDF) of vehicle headway distance. It is shown that the PDF of the headway distance matches well with an exponential distribution, which validates the premise in Subsection III-C.

We then evaluate the data transmission performance for vehicle information collection in VANETs, in terms of the connection probability of a vehicle to an RSU and the end-to-end transmission delay. In Fig. 7, the connection probability is high with the support of VANETs. For instance, the connection probability is 80%, when the vehicle transmission range is set to 120 m, which is very easy to be reached as discussed in [34] and way larger than the average headway distance; and the transmission delay in VANETs is only 5.5 sec. The connection probability increases as the transmission range of vehicle increases, since increasing the transmission range gives more chances to connect with other vehicles or RSUs. Furthermore, these results indicate that given a vehicle-traffic density, RSU deployment and the vehicle transmission range, the connectivity probability can be estimated. Once the estimated connectivity probability is less than the threshold Γ (e.g., $\Gamma = 0.8$), the cellular interface of the heterogeneous wireless network is activated to deliver the vehicular messages instead of VANETs, due to intermittent connectivity. For example, when the vehicles present a decreased transmission range, the connectivity probability may decrease below the threshold, such as the vehicle transmission ranges between 80 and 100 meters.

More importantly, the results show that although the transmission of the heterogeneous network is subject to a delay, the delay is tolerable enough for V2V energy swapping strategy compared with the scheduling period.

C. Evaluation of the Proposed V2V Energy Swapping Strategy

In this subsection, we evaluate the performance of the proposed energy swapping strategy. As a case study, the charging duration is 30 mins (i.e., $\Delta = 0.5$). The period duration τ is 1 hr and the periods cover 24 hours of a day.

1) For the high demand case: We first investigate the performance of the proposed V2V energy swapping strategy under the high demand case. Fig. 8 shows the performance of

This article has been accepted for publication in a future issue of this journal, but has not been fully edited. Content may change prior to final publication. Citation information: DOI 10.1109/TSG.2016.2593667, IEEE Transactions on Smart Grid

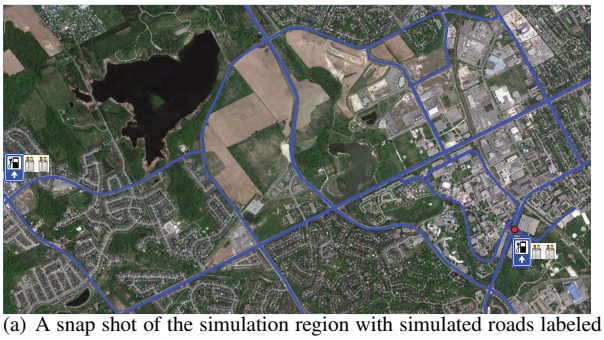

(a) A snap shot of the simulation region with simulated roads labeled in blue.

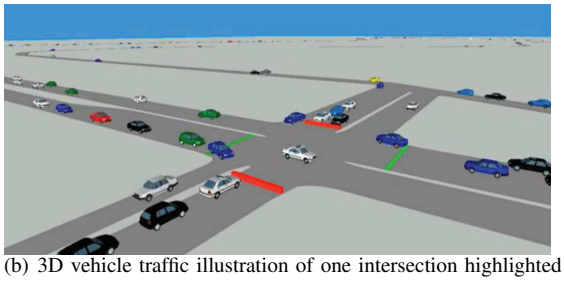

(b) 3D vehicle traffic illustration of one intersection highlighted in red in (a).

Fig. 5: Simulation scenario of University of Waterloo region in VISSIM.

TABLE I: Example of active and reactive power values at each connection point of the system

Hour	Connection Point Number	2	3	4	5	6	7	8	9	10	11	12
21:00	P(MW)	TBD	4.0	5.5	-	6.0	5.5	4.5	-	3.5	TBD	3.0
	Q(MVar)	-	3.0	5.5	-	1.5	5.5	4.5	-	3.0	-	1.5

TABLE II: Normalized power over the power at 21:00 for all the connection points without GEV charging load

Hour	1:00	2:00	3:00	4:00	5:00	6:00	7:00	8:00	9:00	10:00	11:00	12:00
Normalized Power	0.5	0.5	0.5	0.5	0.7	0.9	1.3	1.5	2.1	2.3	2.5	2.5
Hour	13:00	14:00	15:00	16:00	17:00	18:00	19:00	20:00	21:00	22:00	23:00	24:00
Normalized Power	2.5	2.3	2.1	1.8	1.5	1.4	1.3	1.2	1.0	0.7	0.7	0.7

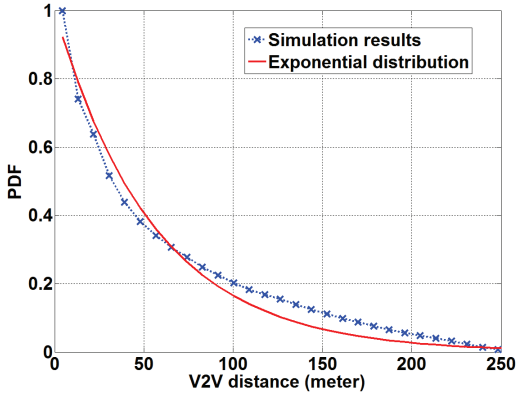

Fig. 6: PDF of vehicle headway distance.

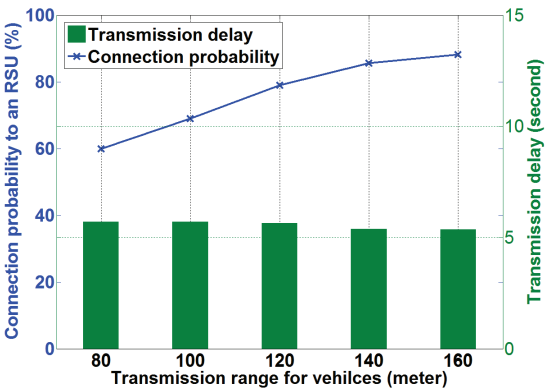

Fig. 7: Data transmission performance in VANETs.

the supply side, given a fixed demand, which is always higher than the supply. Fig. 8(a) shows the total discharged energy from the supplying GEVs, and electricity price for discharging, varying with the total number of vehicles in the supply group. Fig. 8(b) shows the average discharged energy and average reward per supplying GEV. From Fig. 8(a), it can be seen that with the increasing number of supplying vehicles, the total supplied energy increases, and therefore, the electricity price drops. From Fig. 8(b), it can be observed that the average discharged energy per GEV first increases then decreases. Before the point 220, based on a limited number of supplying GEVs, the total number of supplying GEVs is far insufficient. Each GEV has to increase the discharged energy as much as possible to maximize its own revenue. But after 220, as more and more supplying GEVs are involved, the total discharged energy increases. For example, with 280 supplying GEVs, if the average discharged energy still keeps at a higher level, the revenue for individual GEVs is not optimal due to the decreasing electricity price. In this situation, the supplying GEVs can decide relatively smaller individual discharged energy while deciding an optimal electricity price to optimize the individual revenue through negotiation. Besides, the average reward per GEV decreases with an increasing number of supplying GEVs due to the reduced electricity price.

Fig. 9 shows TADE at the demand side under the proposed strategy and the benchmark in [6] for weekday daily profile. The number of supplying GEVs is fixed and only the load capacity at the aggregators varies on a hourly basis, which can be estimated based on the regular loads. The total number of vehicles in the demand group is set to 600, and in the supply group there are 340 GEVs. The black line represents the maximum total available energy from both the supplying GEVs and the grid. First, it can be observed that the total

This article has been accepted for publication in a future issue of this journal, but has not been fully edited. Content may change prior to final publication. Citation information: DOI 10.1109/TSG.2016.2593667, IEEE Transactions on Smart Grid

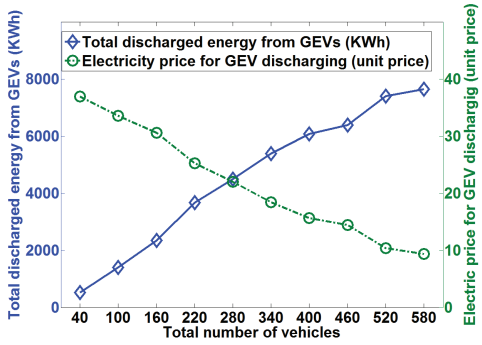

(a) Total supplied energy vs. electricity price.

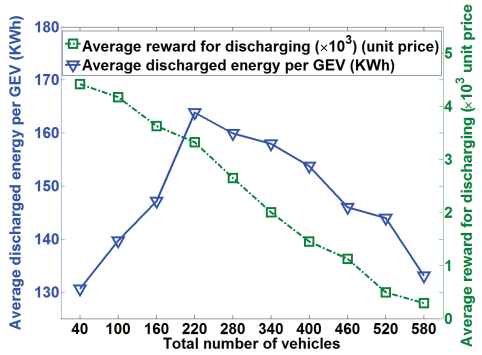

(b) Average discharging rewards vs. Average supplied energy.

Fig. 8: Tradeoff between the supplied energy and the rewards for supplying GEVs.

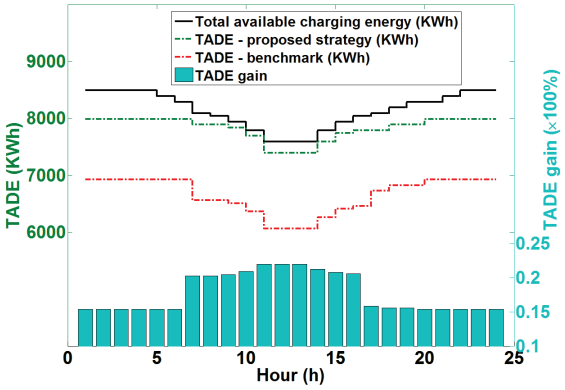

Fig. 9: TADE comparison in daily profile for demanding GEVs.

amount of charging energy under the proposed strategy is considerably higher than that under the benchmark with a 15%-22% gain. Since the benchmark strategy does not collect real-time vehicle information and does not implement spatial coordinations, the charging decisions are made without considering the GEV mobility and the travel cost. As a result, some GEVs may be dispatched to an aggregator that is too far to reach based on their current battery levels, making GEV batteries get depleted on the way and fail to be charged. On the contrary, the proposed strategy considers the travel cost based on the vehicle information collected through the hetergeneous wireless network and dispatches the GEVs only

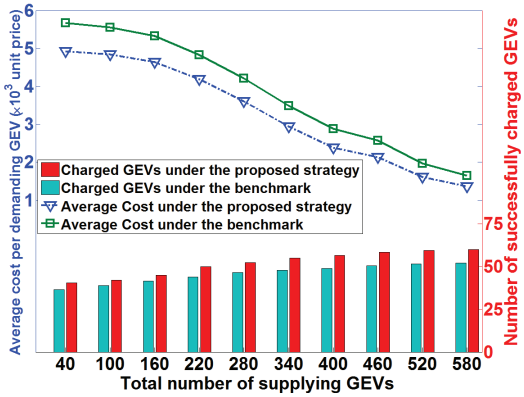

Fig. 10: Number of supplying GEVs vs. average charging cost and number of successfully charged GEVs.

to the aggregators within their reach, thus having a larger TADE. Besides, before 6:00 am, the TADE does not change with time. This is because the total available energy before 6:00 am is sufficient to charge all the demanding GEVs. Between 7:00 am and 8:00 pm, the gap between black line and green line becomes larger when the grid electricity price is higher. For example, the gap at 10:00 am is smaller than that at 1:00 pm, as the grid price at 1:00 pm is higher. The price is announced by the supplying side and delivered to the demanding GEVs via the heterogeneous wireless network.

Fig. 10 shows the relationship among the total number of vehicles in the supply group, the average demanding GEV charging cost, and the number of successfully charged GEVs. The total number of GEVs in the demand group is 600. It can be seen that the average charging cost under both strategies decreases due to a decreased electricity price at the supply side. Besides, the average cost under the proposed strategy is smaller than that for the benchmark due to the smaller average travel cost incurred by the demanding GEVs. In addition, the total number of successfully charged GEVs under the proposed strategy is larger than that for the benchmark, due to the spatial coordination and considering the GEVs' range anxieties.

2) For the surplus supply case: Fig. 11 shows the results on both supply and demand sides in the surplus supply case. The total number of potential supplying GEVs is fixed to 600. It can be observed that the electricity price decreases with the total number of demanding GEVs. This is because more demanding GEVs require more charging energy, and the supplying GEVs will lower the price in order to sell more electricity. Besides, the average reward per discharged GEV first increases and then decreases. This behavior is due to the price drop which is not that large at the beginning. Thus, the increase of discharged energy per supplying GEV brings more rewards. Then, the decrease in electricity price becomes dominant, resulting in a decrease in the average reward per supplying GEV. In addition, the average cost per demanding GEV decreases due to the decrease of price.

VII. Conclusions and Future Work

In this paper, we have proposed a V2V energy swapping strategy based on a HetNet-enhanced smart grid. A mobility-

This article has been accepted for publication in a future issue of this journal, but has not been fully edited. Content may change prior to final publication. Citation information: DOI 10.1109/TSG.2016.2593667, IEEE Transactions on Smart Grid

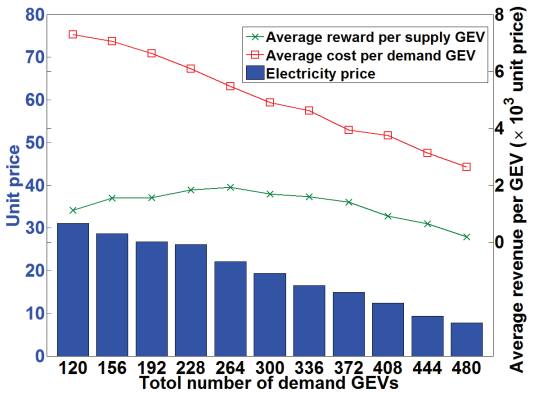

Fig. 11: Performance evaluation in surplus supply case.

aware coordinated V2V energy swapping strategy has been proposed based on a price control mechanism to maximize the discharging revenues for supplying GEVs and minimize the charging cost for demanding GEVs while avoiding power system overload. Extensive simulations have demonstrated that the proposed strategy can achieve better performance than the benchmark in terms of the total GEV charging power, average GEV travel cost, and the number of successfully charged GEVs. In our future work, we intend to incorporate large power system test and large-scale real-world vehicle traffic traces to further validate the benefits of the proposed strategy in practical scenarios. In addition, we will involve the phase unbalanced problem in our future work.

APPENDIX

Proof of Theorem 1: If the Nash equilibrium exists for the set of supplying GEVs in the high demand case, for each supplying GEV, two variables, i.e., $P_{s,a,k}$ and $I_{s,a,k}$ $(=1)$, can be obtained to maximize the GEV revenue. Assume that for GEV s, based on $I_{s,a,k}$, the assigned aggregator in period k is aggregator a, and is **not** the nearest aggregator to GEV s. Meanwhile, the decision variables $P_{s,a,k}$ and $I_{s,a,k}$ should satisfy the corresponding constraints, with the revenue $R_{s,k}$.

However, if we define the nearest aggregator a' to the same GEV s, $P_{s,a',k}(=P_{s,a,k})$ and $I_{s,a',k}(=1$, meanwhile $I_{s,a,k}=0)$ are still feasible for the original problem (13) and satisfy all the associated constraints. The reason is that there is no additional power constraint due to the capacity of the aggregator from the power grid, since in the high demand scenario, the demanding GEVs will consume all the collected energy in the second step and no additional energy will be fed back to the power grid. Hence, for GEV s, if a given discharging power in a faraway aggregator is feasible, the same discharging power in a nearer aggregator is also feasible, yet with a better revenue for that GEV s, $R_{s',k}$, can be obtained due to a shorter travel distance for discharging.

REFERENCES

[1] TESLA Motors, http://www.teslamotors.com/Pages/goelectric#.
[2] N. Mehboob, C. Canizares, and C. Rosenberg, "Day-ahead dispatch of PEV loads in a residential distribution system," *Proc. PES General Meeting*, National Harbor, MD, July 2014.
[3] C. Canizares and J. Nathwani "Towards an Ontario action plan for Plug-In-Electric Vehicles (PEVs)," Waterloo Inst. Sustain. Energy, Univ. Waterloo, Waterloo, ON, Canada, Tech. Rep., 2010. [Online]. Available: https://wise.uwaterloo.ca/documents/experts/claudiocanizares/public/ phev-report-may-17pdf.
[4] M. Tabari and A. Yazdani, "An energy management strategy for a DC distribution system for power system integration of Plug-In Electric Vehicles," *IEEE Trans. on Smart Grid*, vol. 7, no. 2, pp. 659-668, 2016.
[5] H. Liang, B. J. Choi, W. Zhuang, and X. Shen, "Optimizing the energy delivery via V2G systems based on stochastic inventory theory," *IEEE Trans. on Smart Grid*, vol. 4, no. 4, pp. 2230-2243, 2013.
[6] P. Richardson, D. Flynn, and A. Keane, "Local versus centralized charging strategies for electric vehicles in low voltage distribution systems," *IEEE Trans. on Smart Grid*, vol. 3, no. 2, pp. 1020-1028, 2012.
[7] C. Liu, K. Chau, D. Wu, and S. Gao, "Opportunities and challenges of vehicle-to-home, vehicle-to-vehicle, and vehicle-to-grid technologies," *Proc. of The IEEE*, vol. 101, no. 11, pp. 2409-2427, 2013.
[8] M. Sarker, H. Pandzic, and M. Ortega-Vazquez, "Optimal operation adn services scheduling for an electric vehicle battery swapping station," *IEEE Trans. on Power Systems*, vol. 30, no. 2, pp. 901-910, 2015.
[9] IEEE WG, *IEEE 802.11p/D2.01, Draft Amendement to Part 11: Wireless Medium Access Control (MAC) and Physical Layer (PHY) specifications: Wireless Access in Vehicular Environments*, Mar. 2007.
[10] L. Gan, U. Topcu, and S. Low, "Optimal decentralized protocol for EV charging," *IEEE Trans. on Power Systems*, vol. 28, no. 2, pp. 940-951, 2013.
[11] J. Friedman, Oligopoly and the theory of games, *North Holland Publishing Company*, 1977.
[12] S. Boyd and L. Vandenberghe, *Convex Optimization,* Cambridge, U.K., Cambridge Univ. Press, 2004.
[13] M. Duran and I. Grossmann, "An outer-approximation algorithm for a class of mixed-integer nonlinear programs," *Mathematical Programming*, vol. 36, no. 3, pp. 307-339, 1986.
[14] http://vision-traffic.ptvgroup.com/en-uk/products/ptv-vissim/.
[15] Y. Cao, S. Tang, C. Li, P. Zhang, Y. Tan, Z. Zhang, and J. Li, "An optimized EV charging model considering TOU price and SOC curve," *IEEE Trans. on Smart Grid*, vol. 3, no. 1, pp. 388-393, 2012.
[16] M. F Shaaban, M. Ismail, E. F. El-Saadany, and W. Zhuang, "Real-time PEV charging/discharging coordination in smart distribution systems," *IEEE Trans. on Smart Grid*, vol. 5, no. 4, pp. 1797-1807, 2014.
[17] M. Wang, M. Ismail, X. Shen, E. Serpedin, and K. Qaraqe "Spatial and temporal online charging/discharging coordination for mobile PEVs," *Proc. IEEE Globecom*, Austin, US, Dec. 2014.
[18] M. Wang, M. Ismail, R. Zhang, X. Shen, E. Serpedin, and K. Qaraqe, "Mobility-aware coordinated charging for electric vehicles in VANET-enhanced smart grid", *IEEE Wireless Communications Magazine*, vol. 22, no. 1, pp. 112-121, 2015.
[19] D. Wu, K. Chau, and S. Gao, "Multilayer framework for vehicle-to-grid operation," *Proc. IEEE Vehicle Power and Propulsion Conf.*, Lille, Sept. 2010.
[20] A. Abdrabou and W. Zhuang, "Probabilistic delay control and road side unit placement for vehicular ad hoc netowrks with disrupted connectivity," *IEEE J. Sel. Areas Comm.*, vol. 29, no. 1, pp. 129-139, 2011.
[21] A. May, *Traffic flow fundamentals*, Prentice Hall, 1990.
[22] N. Wisitpongphan, F. Bai, P. Mudalige, V. Sadekar, and O. Tonguz, "Routing in sparse vehicular ad hoc networks," *IEEE J. Sel. Areas Comm.*, vol. 25, no. 8, pp. 1538-1556, 2007.
[23] https://www.canadatransformers.com/transformer-efficiency-losses-heat/
[24] M. Shaaban, M. Ismail, E. El-Saadany, and W. Zhuang, "Real-time PEV charging/dicharging coordination in smart distribution systems," *IEEE Trans. on Smart Grid*, vol. 5, no. 4, pp. 1797-1807, 2014.
[25] M. Khodayar, L. Wu, and M. Shahidehpour, "Hourly coordination of electric vehicle operation and volatile wind power generation in SCUC," *IEEE Trans. on Smart Grid*, vol. 3, no. 3, pp. 1271-1279, 2012.
[26] M. E. Elkhatb, R. El-Shatshat, and M. Salama, "Novel coordinated voltage control for smart distribution network with DG," *IEEE Trans. on Smart Grid*, vol. 2, no. 4, pp. 598-605, 2011.
[27] R. Nelson, "Power requirements for batteries in hybrid electric vehicles", *IEEE Journal of Power Source*, vol. 91, no. 1, pp. 2-26, Nov. 2000.
[28] T. Kristoffersen, K. Capion, and P. Meibom, "Optimal charging of electric drive vehicles in a market environment," *Journal of Applied Energy*, vol. 88, no. 5, pp. 1940-1948, 2011.
[29] M. Abboud, L. Jaoude, and Z. Kerbage, "Real time GPS navigation system," http://webfea-lb.fea.aub.edu.lb/proceedings/2004/SRC-ECE-27.pdf, 2004.
[30] A. Geoffrion, "Lagrangean relaxation for integer programming," *Mathematical Programming Study*, vol. 2, pp. 82-114, 1974.
[31] P. Bonami, L. Biegler, A. Conn, G. Cornue, I. Grossmann, C. Laird, J. Lee, A. Lodi, F. Margot, N. Sawaya, and A. Wachter, "An algorithmic framework for convex mixed integer nonlinear programs," *Discrete Optimization*, vol. 5, no. 2, pp. 186-204, 2008.
[32] C. Norén and J. Pyrko, "Typical load shapes for Swedish schools and hotels," *Energy and Buildings*, vol. 28, no. 2, pp. 145-157, 1998.
[33] R. Wiedemann, "Modeling of RTI-elements on multi-lane roads," *Proc. Drive Conference*, Brussels, Belgium, Feb. 1991.
[34] L. Cheng, B. E. Henty, D. D. Stancil, F. Bai, and P. Mudalige, "Mobile vehicle-to-vehicle narrow-band channel measurement and characterization of the 5.9 GHz dedicated short range communication (DSRC) frequency band," *IEEE J. Sel. Areas Comm.*, vol. 25, no. 8, pp. 1501-1516, 2007.

This article has been accepted for publication in a future issue of this journal, but has not been fully edited. Content may change prior to final publication. Citation information: DOI 10.1109/TSG.2016.2593667, IEEE Transactions on Smart Grid

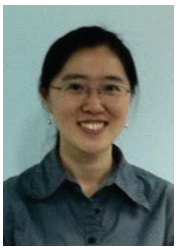

Miao Wang received her B.Sc. degree from Beijing University of Posts and Telecommunications and M.Sc. degree from Beihang University, Beijing, China, in 2007 and 2010, respectively, and the Ph.D. degree in electrical and computer engineering from the University of Waterloo, Waterloo, ON, Canada, in 2015. She is currently working as the postdoctoral fellowship with the Department of Electrical and Computer Engineering, University of Waterloo, Waterloo, ON, Canada. Her current research interests include electric vehicles charing/discharging strategy design in smart grid, traffic control, capacity and delay analysis, and routing protocol design for vehicular networks.

Muhammad Ismail (S'10-M'13) received the B.Sc. and M.Sc. degrees in electrical engineering (electronics and communications) from Ain Shams University, Cairo, Egypt, in 2007 and 2009, respectively, and the Ph.D. degree in electrical and computer engineering from the University of Waterloo, Waterloo, ON, Canada, in 2013. He is an Assistant Research Scientist with the Department of Electrical and Computer Engineering, Texas A&M University at Qatar, Doha, Qatar. His research interests include distributed resource allocation, green wireless networks, cooperative networking, smart grid, and biomedical signal processing. He is a co-recipient of the Best Paper Award at IEEE ICC 2014 and IEEE Globecom 2014.

Ran Zhang received his B.E. degree (2010) from Tsinghua University (China) in Electronics Engineering, and the Ph.D. degree in electrical and computer engineering from the University of Waterloo, Waterloo, ON, Canada, in 2016. His current research interest includes electrical vehicle charging control in smart grids, resource management in heterogeneous wireless access networks, and carrier aggregation in Long Term Evolution - Advanced (LTEA) systems.

Xuemin (Sherman) Shen (IEEE M'97-SM'02-F09) is a Professor and University Research Chair, Department of Electrical and Computer Engineering, University of Waterloo, Canada. His research focuses on resource management, wireless network security, social networks, smart grid, and vehicular ad hoc networks. He is an elected member of IEEE ComSoc Board of Governor, and the Chair of Distinguished Lecturers Selection Committee. Dr. Shen served as the Technical Program Committee Chair/Co-Chair for IEEE Globecom16, Infocom14, IEEE VTC10 Fall, and Globecom07, the Symposia Chair for IEEE ICC10, the Tutorial Chair for IEEE VTC11 Spring and IEEE ICC08, the General Co-Chair for ACM Mobihoc15, the Chair for IEEE Communications Society Technical Committee on Wireless Communications. He also served/serves as the Editor-inChief for IEEE Network, Peer-to-Peer Networking and Application, and IET Communications; a Founding Area Editor for IEEE Transactions on Wireless Communications. Dr. Shen received the Excellent Graduate Supervision Award in 2006, and the Outstanding Performance Award from the University of Waterloo, and the Premiers Research Excellence Award (PREA) in 2003 from the Province of Ontario, Canada. Dr. Shen is a registered Professional Engineer of Ontario, Canada, a Fellow of IEEE, Engineering Institute of Canada, Canadian Academy of Engineering, and Royal Society of Canada, and a Distinguished Lecturer of IEEE Vehicular Technology Society and Communications Society.

Erchin Serpedin (F'13) is a Professor with the Department of Electrical and Computer Engineering, Texas A&M University, College Station, TX, USA. He received the specialization degree in signal processing and transmission of information from Ecole Superieure DElectricite (SUPELEC), Paris, France, in 1992, the M.Sc. degree from the Georgia Institute of Technology, Atlanta, USA, in 1992, and the Ph.D. degree in electrical engineering from the University of Virginia, Charlottesville, USA, in January 1999. Dr. Serpedin is the author of 2 research monographs, 1 textbook, 9 book chapters, 110 journal papers, and 180 conference papers. His research interests include signal processing, biomedical engineering, bioinformatics, and machine learning. Dr. Serpedin is currently serving as an Associate Editor of the IEEE SIGNAL PROCESSING MAGAZINE and as the Editor-in-Chief of the journal EURASIP Journal on Bioinformatics and Systems Biology, an online journal edited by Springer. He served as an Associate Editor of a dozen of journals, such as the IEEE TRANSACTIONS ON INFORMATION THEORY, IEEE TRANSACTIONS ON SIGNAL PROCESSING, IEEE TRANSACTIONS ON COMMUNICATIONS, IEEE SIGNAL PROCESSING L ETTERS, IEEE COMMUNICATIONS LETTERS, IEEE TRANSACTIONS ON WIRELESS COMMUNICATIONS, Signal Processing (Elsevier), Physical Communications (Elsevier), EURASIP Journal on Advances in Signal Processing, and as a Technical Chair for five major conferences. He was a recipient of numerous awards and research grants.

Khalid Qaraqe (M'97-SM'00) was born in Bethlehem. He received the B.S. degree (with honors) from the University of Technology, Baghdad, Iraq, in 1986, the M.S. degree from the University of Jordan, Amman, Jordan, in 1989, and the Ph.D. degree in electrical from Texas A&M University, College Station, TX, USA, in 1997, all in electrical engineering. From 1989 to 2004, he held a variety positions in many companies, and he has over 12 years of experience in the telecommunication industry. He has worked for Qualcomm, Enad Design Systems, Cadence Design Systems/Tality Corporation, STC, SBC, and Ericsson. He has worked on numerous GSM, CDMA, and WCDMA projects and has experience in product development, design, deployments, testing, and integration. He joined the Department of Electrical and Computer Engineering, Texas A&M University at Qatar, Doha, Qatar, in July 2004, where he is currently a Professor. His research interests include communication theory and its application to design and performance, analysis of cellular systems, and indoor communication systems. His particular interests are in mobile networks, broadband wireless access, cooperative networks, cognitive radio, diversity techniques, and beyond 4G systems.